Eighth Quarterly Progress Report

October 1, 2003, through December 31, 2003

Speech Processors for Auditory Prostheses

NIH Contract N01-DC-2-1001

submitted by

Barbara Herrmann
Massachusetts Eye and Ear Infirmary
Audiology Department
Boston, MA

Charles C. Finley
University of North Carolina at Chapel Hill
Department of Otolaryngology
Chapel Hill, NC

Donald K. Eddington
Massachusetts Institute of Technology
Research Laboratory of Electronics
Cambridge, MA

1.0 Introduction

Work performed with the support of this contract is directed at the design, development, and evaluation of sound-processing strategies for auditory prostheses implanted in deaf humans. The investigators, engineers, audiologists and students conducting this work are from four collaborating institutions: the Massachusetts Institute of Technology (MIT), the Massachusetts Eye and Ear Infirmary (MEEI), Boston University (BU) and the University of North Carolina at Chapel Hill (UNC-CH). Major research efforts are proceeding in four areas: (1) developing and maintaining a laboratory-based, software-controlled, real-time stimulation facility for making psychophysical measurements, recording field and evoked potentials and implementing/testing a wide range of monolateral and bilateral sound-processing strategies, (2) refining the sound processing algorithms used in current commercial and laboratory processors, (3) exploring new sound-processing strategies for implanted subjects, and (4) understanding factors contributing to the wide range of performance seen in the population of implantees through psychophysical, evoked-response and fMRI measures.

This quarter's efforts were directed at seven main areas that include: 1) studies of sound localization and speech reception in the presence of multiple noise sources using asynchronous sound-processing systems, 2) initiation of preparations to conduct similar experiments using synchronized sound processors, 3) continued monitoring of the relationships of pitch, fusion, ITD-JND, and binaural interactions in electrically-evoked brainstem responses, 4) fitting of additional chronic study subjects wearing CIS-based processors whose channel interactions have been minimized using triphasic pulses, 5) continued development and expansion of device testing using surface-artifact potentials, 6) continued measurement and analysis of intracochlear evoked potentials (IEPs) to characterize the quality, magnitude and variability of this measure across a pool of subjects, and 7) investigations of channel interaction using the IEP which we will eventually compared to psychophysical measures of interaction. In this QPR, we concentrate on the measurement and initial analysis of channel interaction using the IEP and describe the fast-recovery amplifier developed to record electrically-evoked, potentials recorded from intracochlear and surface electrodes. The amplifier is also used to record stimulus artifact potentials from intracochlear or surface electrodes.

2.0 **IEP Measures of Channel Interaction**

As reported in the fourth quarter report of this project (Finley et al., 2002), custom software has been developed and used to record evoked neural potentials from intracochlear electrodes of the Clarion CII\HiFocus implant system. Subjects are post-lingually deaf monolaterally-implanted Clarion patients with a wide range of speech-reception performance (0% to 82% CNC word scores). Data collected include 1) the growth of the IEP amplitude (aIEP) as a function of increasing stimulus level for an apical (E3), middle (E7) and basa1 (E13) electrode and 2) aIEP as a function of the intracochlear recording electrode for a fixed stimulation electrode and current level. We continue to observe inter subject variability in both measures as illustrated by Figures 1A and 1B which show the growth functions (Figure 1A) and spatial distributions (Figure 1B) of the aIEP for stimulation of E7 in 10 subjects .

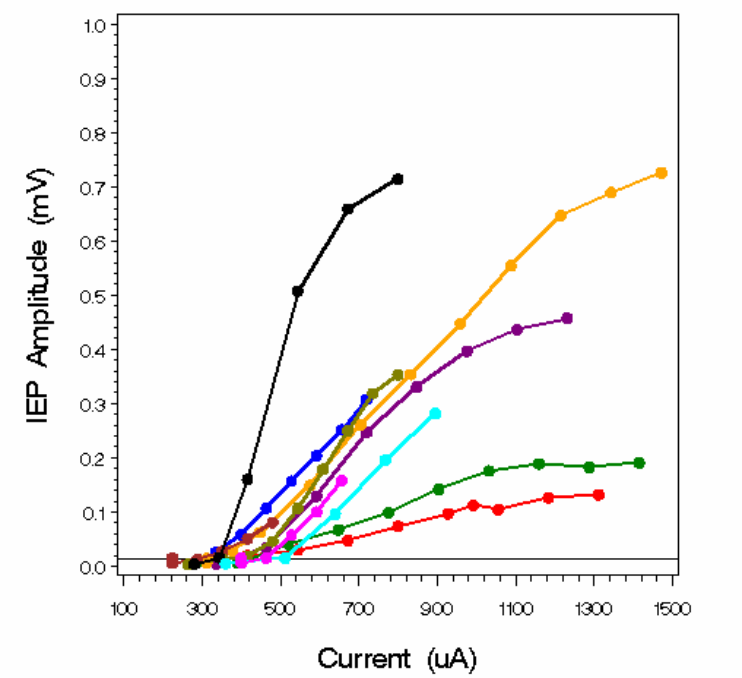

Figure 1A. IEP amplitude (aIEP) as a function of stimulus level at electrode E7 (recording electrode E5) for 10 subjects.

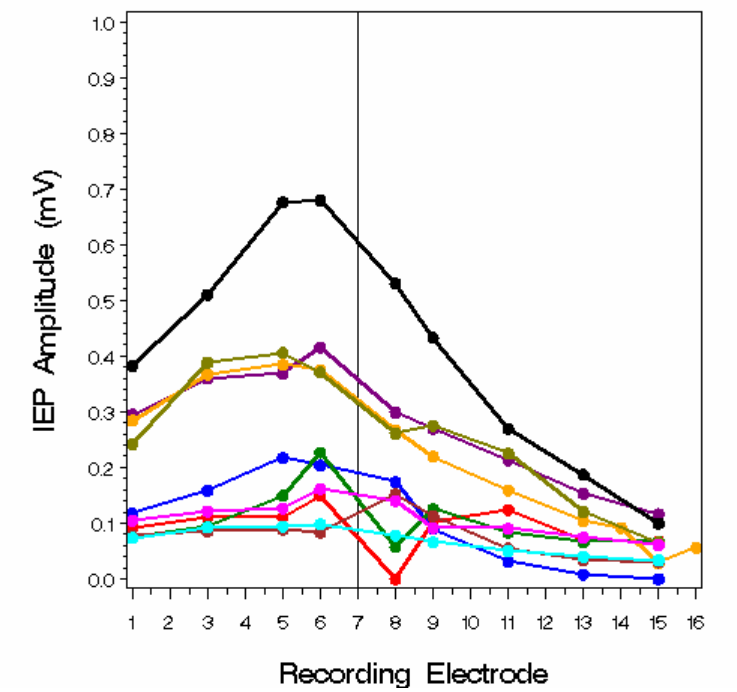

Figure 1B. Plots of aIEP as a function of recording electrode (aIEP spatial distribution) for stimulating Electrode 7 in 10 subjects. Stimulating current was fixed for each subject near the maximal aIEP measured while collecting the I/O function.

In addition to these IEP measures, we have also modified our software to be able to stimulate more than one electrode at a time while still recording the IEP from an arbitrary, unstimulated

intracochlear electrode. This has given us the capability to explore channel interaction effects using the IEP by examining the change in the aIEP to a single electrode *probe* stimulus while additional *masker* current is applied to another electrode. In order to simplify our initial exploration of IEP interaction, we use masker levels well below those eliciting an IEP when applied to the masker electrode alone (i.e. below IEP threshold). By using these low masker levels, we do not need to account for the effects of the "masker alone" condition in interpreting our results. We also maximized the likelihood of observing interaction by presenting the masker and probe signals simultaneously. Finally, we investigated the effect of phase by using maskers that were both in-phase and 180 degrees out-of-phase with the biphasic pulse used on the probe electrode. Studies employing non-simultaneous masker and probe stimulation that more closely mimic conditions occurring during realistic speech processor operation are planned for the future.

2.1 **IEP Interaction Procedure**

Figure 2A is an example of an IEP response to an alternating polarity 32 usec/phase biphasic pulse applied to a single electrode. The measurement used to characterize the amplitude of this response (aIEP) is the amplitude difference between the initial negative peak after the stimulus artifact (N1) to the following positive peak (P2). Although the slope of the I/O function for this response varies across subjects as illustrated previously (Figure 1A), the measurement variability is small when repeated within a subject (Figure 2B)

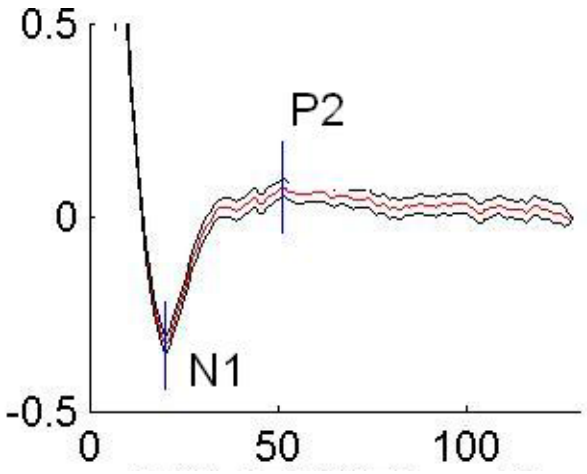

Figure 2A. Example of an averaged IEP recording. The center trace is the amplitude average of 256 data vectors and the traces on either side mark the 95% confidence intervals. The difference P2-N1 corresponds to the IEP amplitudes (aIEPs) plotted in subsequent figures. The horizontal axis represents the sample points of the record (sampling rate 60.975 kHz) and the vertical axis indicates aIEP in mV.

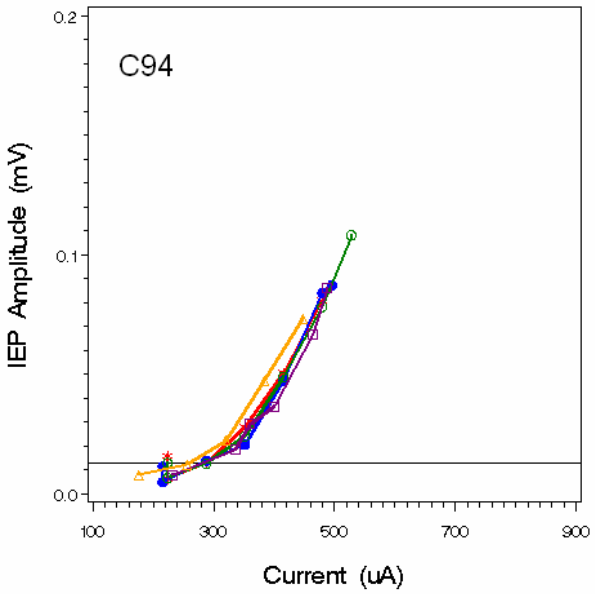

Figure 2B. Repeated measures of the I/O function for E 7 in one subject measured on separate days

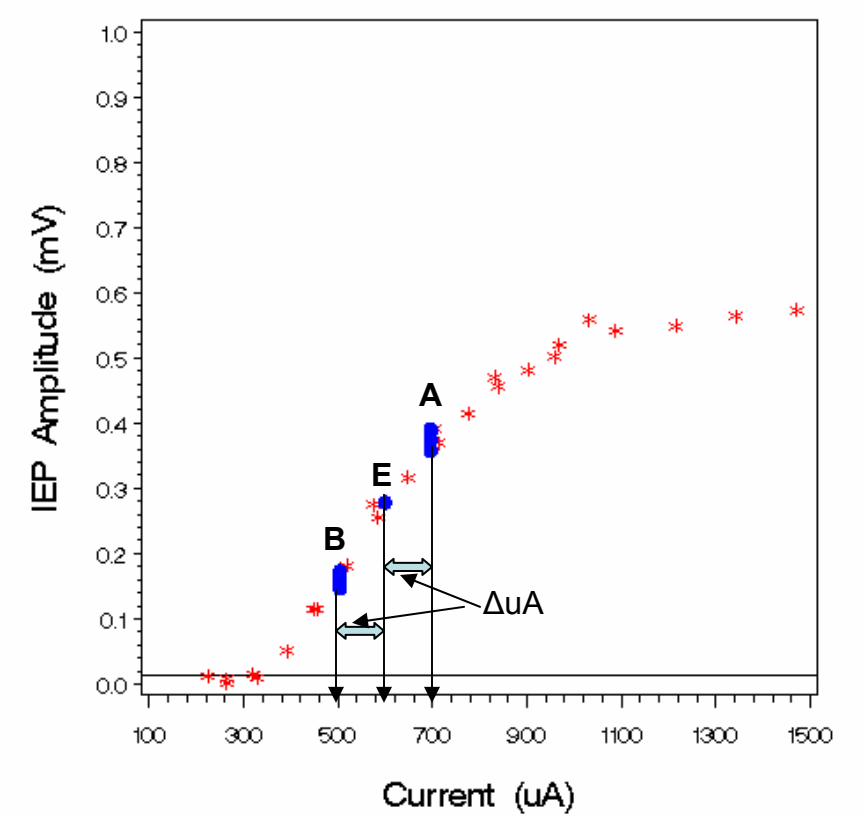

Figure 3. I/O function (stars) plotted together with the aIEPs measured for three stimulus conditions used by the interaction procedure (dots) for probe electrode E3 of one subject. Point E is the aIEP elicited by the base current on the probe electrode alone. Point A is the aIEP elicited when ΔuA is added in-phase to the base current on the probe (current is increased on probe electrode). Point B is IEP amplitude when ΔuA is applied 180 degrees out-of-phase to the base current on the probe (current is decreased on probe electrode). In this example, ΔuA is 96 uA which is well below both IEP and psychophysical threshold for this subject on all electrodes. Multiple measures are plotted for aIEP for conditions A and E.

To examine the effect of a subthreshold masker on the IEP, we measured the I/O function for a probe stimulus (Figure 3) and then chose a point on the relatively linear portion of that function (the base level) where a change in current (ΔuA) in either direction changed the amplitude of the IEP (aIEP) and where ΔuA was below the IEP threshold for both the masker and probe electrodes when stimulated alone.

As summarized in the following table, IEPs were recorded for four experimental conditions for each probe-masker combination (Conditions A,B,C,D) and for the probe electrode stimulated alone at base level (Condition E).

Condition	Probe Electrode Stimulus	Masker Electrode Stimulus
A	Base uA + ΔuA (in-phase)	0
B	Base uA – ΔuA (out-of-phase)	0
C	Base uA	ΔuA (in-phase)
D	Base uA	ΔuA (out-of-phase)
E	Base uA	0

In condition A, the ΔuA stimulus was added in-phase to the base stimulus on the probe itself resulting in an increase in the probe stimulus level. Consequently, the aIEP for condition A ($aIEP_A$) was greater than for condition E (i.e., $aIEP_A > aIEP_E$). The ΔuA stimulus was added out-of-phase to the base stimulus on the probe in condition B, decreasing the current magnitude on the probe electrode and resulting in a smaller $aIEP_B$ than $aIEP_E$. In condition C, the base stimulus was applied to the probe electrode and the ΔuA stimulus was applied to a masker electrode in-phase with the probe's base stimulus. In the case of condition D, the base stimulus was applied to the probe electrode and ΔuA was applied to a masker out-of-phase to the probe stimulus. The degree to which $aIEP_C$ and $aIEP_D$ differ from $aIEP_E$ depends on the degree of interaction between the probe and masker electrodes. The comparison of $aIEP_C$ to $aIEP_A$ and $aIEP_D$ to $aIEP_B$ contrasts the interaction between the probe and the masker to the simple increase of current on the probe.

Typical IEP responses for these five probe-masker conditions are illustrated in Figure 4 for the following electrode configuration: E7 probe, E13 masker and E5 recording electrode. The base stimulation level was 648 uA peak and the ΔuA stimulation level was 96 uA. Stimulation and recording were both referenced to the banded return electrode on the implanted CII stimulator case.

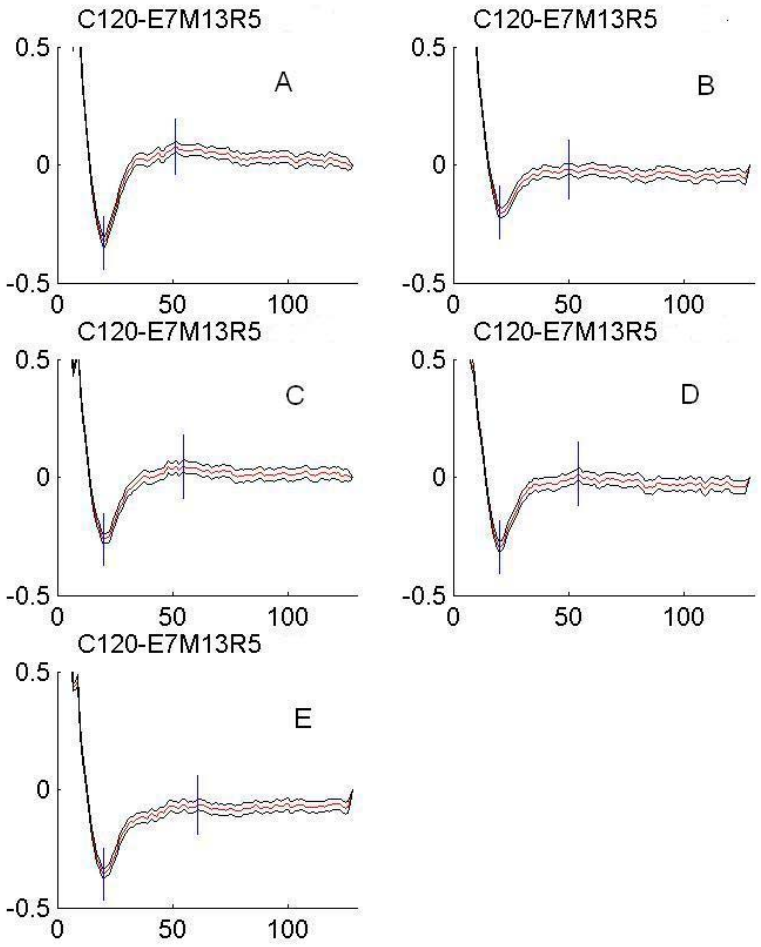

Figure 4. Examples of IEP recordings for the five probe-masker conditions used in the interaction procedure. In condition E, the probe (E7) is stimulated at the base level. The ΔuA stimulus is added in-phase to base current and applied to the probe in condition A and added out-of-phase to the base stimulus when used to stimulate the probe in condition B. In condition C, the base current is applied to the probe (E7) and the ΔuA stimulus is applied to the masker (E13) in-phase with the base stimulus. In condition D, the ΔuA stimulus is applied to the masker (E13) out-of-phase with the probe's base stimulus. The horizontal axes represent sample points (60.975 sampling rate) and the vertical axes indicate aIEP in mV

For the data described in this report, IEP responses were measured for three probe electrodes:, E3 near the apical end of the electrode array, E7 in the middle of the electrode array, and E13 in the basal end. IEP recordings (Conditions A-D) were made for nine probe-masker combinations for each probe electrode. Masker electrodes for each probe include the two electrodes adjacent to the probe plus the odd-numbered electrodes on either side of the probe electrode. For example, for probe E7, masker electrodes were E1, E3, E5, E6, E8, E9, E11, E13 and E15. The recording electrode for the IEP was spaced either two electrodes apical or two electrodes basal to the probe electrode depending upon whether the masker was apical or basal to the probe electrode. If the masker electrode was basal to the probe, the recording electrode apical to the probe was used and vice versa. This selection of recording electrode was made (1) to further simplify interpretation of the recorded IEP data by avoiding potentially complex response

summations occurring in the region between the probe and masker electrodes and (2) to allow uniform recording electrode conditions over a wide range of probe-masker electrode distances, but especially when the masker is near the probe electrode. Because the aIEP was observed to vary depending upon the recording electrode in several subjects, the aIEP for the probe alone at the base stimulus level (Condition E) was recorded for both recording electrode conditions and matched to that used for the measurements of Conditions A–D for each probe-masker combination.

IEP interaction measurements have been made on six adult subjects who were post-lingually deafened. Each had been implanted with a Clarion CII device with the HiFocus electrode (and positioner) and had been using his/her implant for 6 months to 3 years. Speech perception for these six subjects is relatively good with CNC scores ranging from 62% to 82%. All but one subject used a pulsatile processing strategy of either Hi-Resolution S or CIS. One subject uses the SAS processing strategy.

2.2 Analysis of Electrode Interactions Based on IEP Measures

IEP interaction was defined as the change in the aIEP to a probe alone, base-level signal (Condition E) when a subthreshold current was placed on a different masker electrode (Conditions C and D). The aIEPs measured when the subthreshold current (ΔuA) was added directly to the base-level stimulus on the probe itself ($aIEP_A$ for Condition A and $aIEP_B$ for Condition B) are considered reference aIEPs representing conditions of total interaction. Section 2.3.3. below addresses the issue of quantitatively measuring the degree of interaction. This is separate and apart from the question of whether an observed change is statistically different from zero, thus indicating that some level of interaction exists.

In order to make IEP amplitude comparisons in a statistically meaningful way, it was necessary to obtain an estimate of the variance for the aIEPs measured in each condition. Because the aIEP is a derived measure (i.e. calculated from two separate samples), we estimated the aIEP variance by resampling (Efron et al., 1993) the raw data vectors of each IEP average. Specifically, the process was as follows:

1. During data collection, the voltage at the recording electrode was sampled for approximately 2 ms after stimulus onset at a rate of 60 kHz forming an individual data vector of 128 samples. A total of 256 of these data vectors were recorded for each masker/probe condition.
2. The average of the 256 data vectors was computed and visually examined to determine the time latencies of the N1 and P2 responses.
3. The sample values at the N1 and P2 latencies were extracted from each of the 256 data vectors creating a pool of 256 samples for each latency.
4. The two pools were resampled 1000 times with replacement by randomly selecting one sample from each pool, then calculating the N1-P2 difference to produce 1000 estimates of the aIEP. (See Efron et al., 1993 for the theoretical basis supporting the use of the N1 and P2 samples as the best estimate of the N1 and P2 populations for computation of the following statistics).

5. The mean value, variance and 95% confidence limits were then calculated from the 1000 aIEP estimates.
6. Two aIEPs measures were determined to be significantly different when their 95% confidence intervals did not overlap.

The aIEP for conditions A – E with corresponding 95% confidence intervals are shown in Figure 5 for one subject for the following test configuration: probe E7, masker E13, recording E5. In this situation, application of a subthreshold stimulus (ΔuA) on masker E13 did not show a significant effect on the aIEP elicited by the base stimulus on E7 for both the in-phase masker (condition C) and the out-of-phase (Condition D) masker. The same ΔuA stimulus added directly (both in-phase and out-of-phase) to the base stimulus on the probe electrode did change the aIEP significantly (Conditions A and B). Based on these results, we conclude that E13 did not interact with E7.

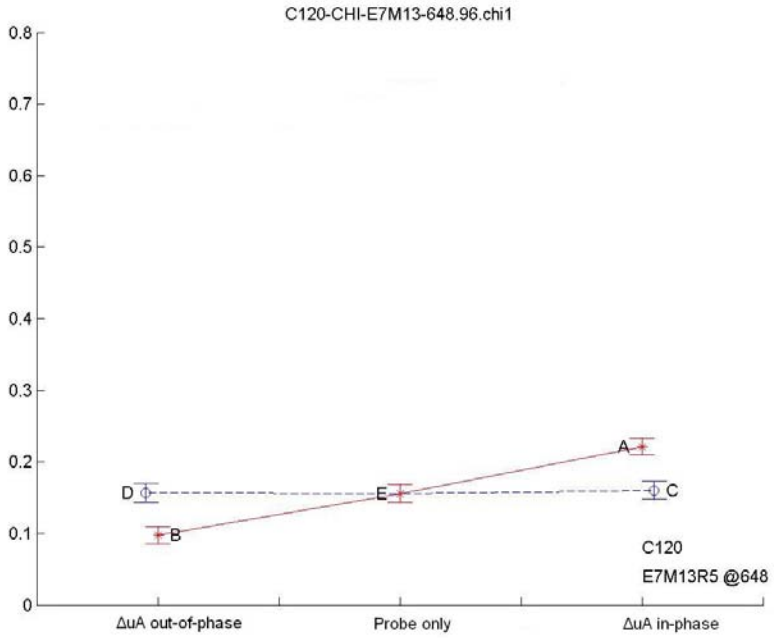

Figure 5. Plot of IEP amplitude and corresponding 95% confidence intervals for the five conditions measured for the masker/probe configuration: probe E7, masker E13 and recording E5. In conditions A, B and E, only on the probe electrode (E7) is stimulated. In conditions C and D, the base current is delivered to the probe (E7) and ΔuA is delivered to the masker electrode (E13) either in phase (C) or out-of-phase (D) with the base current.

2.3 Results of IEP Interaction Analysis:

In order to illustrate the range of interaction patterns we observed, we present four examples in Figure 6.

- The case of no interaction described above and plotted in Figure 5 is reproduced as panel A in Figure 6.
- Panel B shows a case where the change in the aIEP due to the in-phase or out-of-phase use of the ΔuA stimulus was about the same whether it was applied to the probe electrode directly or to the masker electrode (i.e., $aIEP_A \approx aIEP_C$ and $aIEP_B \approx aIEP_D$). This indicates a good deal of interaction because applying the subthreshold stimulus to the masker has about the same impact on the aIEP as adding it directly to the base-level stimulus on the probe.
- In the Panel C case, the impact of the ΔuA stimulus being delivered to the masker electrode depended on whether it was in-phase or out-of-phase with the probe's base-level stimulus. In the out-of-phase case, $aIEP_D$ was less than $aIEP_B$ and about the same as $aIEP_E$ suggesting very little interaction. The in-phase case, however, shows a high degree if interaction with $aIEP_C \approx aIEP_A$.
- The example shown in Panel D was unexpected. In this case, $aIEP_C > aIEP_A$. This means the impact on the aIEP was greater when the below-threshold ΔuA stimulus was delivered (in-phase) to the masker electrode than when it was added directly to the probe stimulus. Following analyses will show this "hyperinteraction" was almost always associated with masker stimuli that were in-phase with the probe signal.

2.3.1 Frequency of IEP Interaction Across Subjects and Probe Electrodes

The frequency of IEP interaction across subjects and across electrodes for in-phase maskers is shown in Figure 7A and for out-of-phase maskers in Figure 7B. Notice that interaction occurs more frequently when a subthreshold masker is in-phase with the probe signal than out-of-phase with the probe signal (66% vs 22% of all combinations showed interaction). The frequency of interaction is also higher for maskers closer to the probe and decreases as masker distance increases.

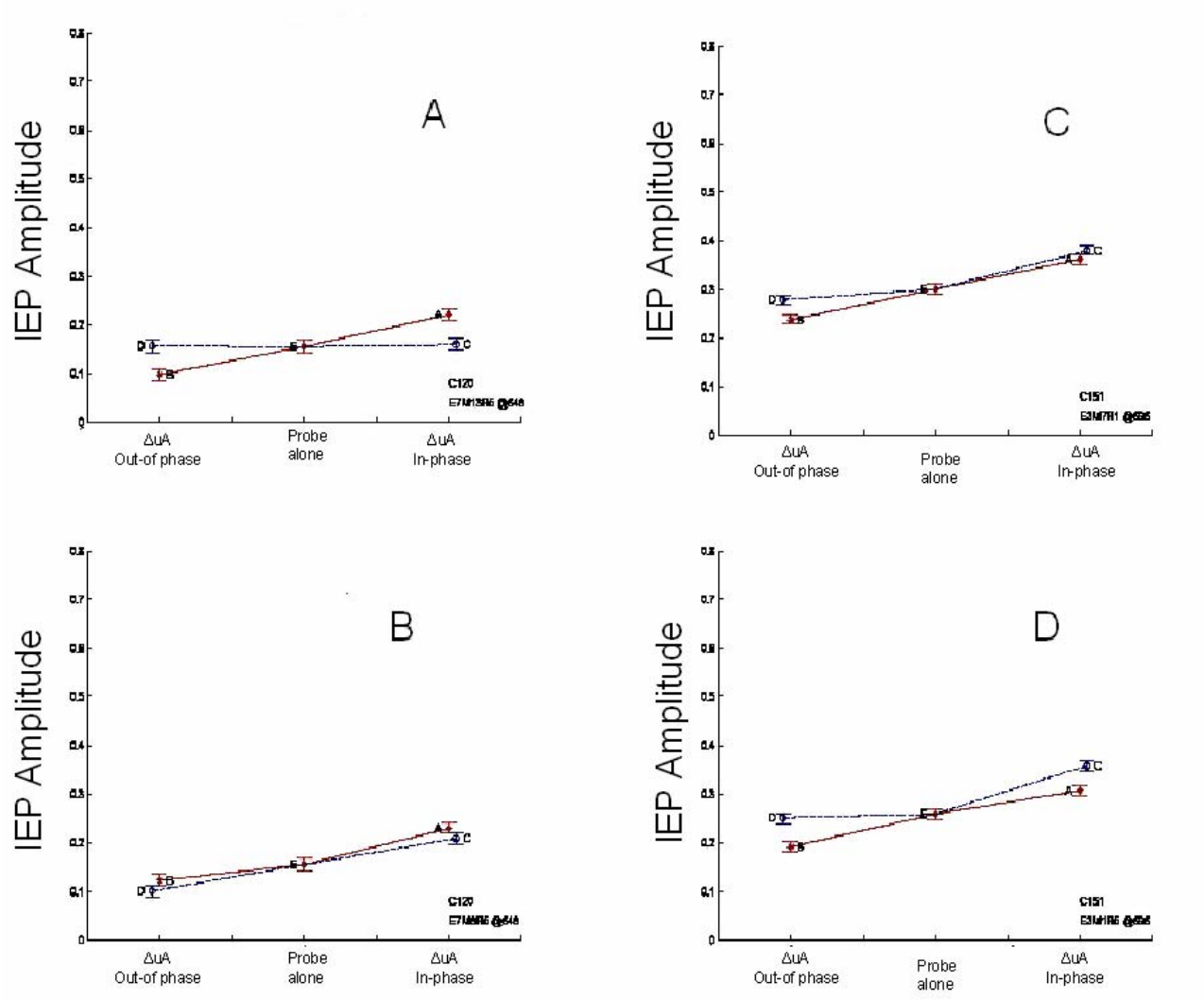

Figure 6. Examples illustrating the range of interaction patterns observed. Panel **A** illustrates no interaction since the aIEP for conditions D and C do not differ significantly from the aIEP of condition E. Panel **B** illustrates a masker effect on aIEP (Conditions C and D) that is similar to that seen when the ΔuA stimulus is applied to the base current on the probe (Conditions A and B). In the case of panel **C**, the interaction effects for the in-phase masker is larger than for the out-of-phase masker stimulus. The in-phase masker (condition C) has a similar effect to applying ΔuA in-phase to the base stimulus on the probe, while an out-of-phase masker does not significantly change the aIEP (e.g., Condition D is not significantly different from Condition E). Panel **D** illustrates an unexpected degree of interaction most often observed for in-phase maskers. Here the ΔuA stimulus on the masker electrode increases aIEP more than if the same change in current was applied directly to the probe electrode (i.e., the aIEP for Condition C is significantly greater than the aIEP for both Condition E and Condition A referred to in the text as "hyperinteraction".

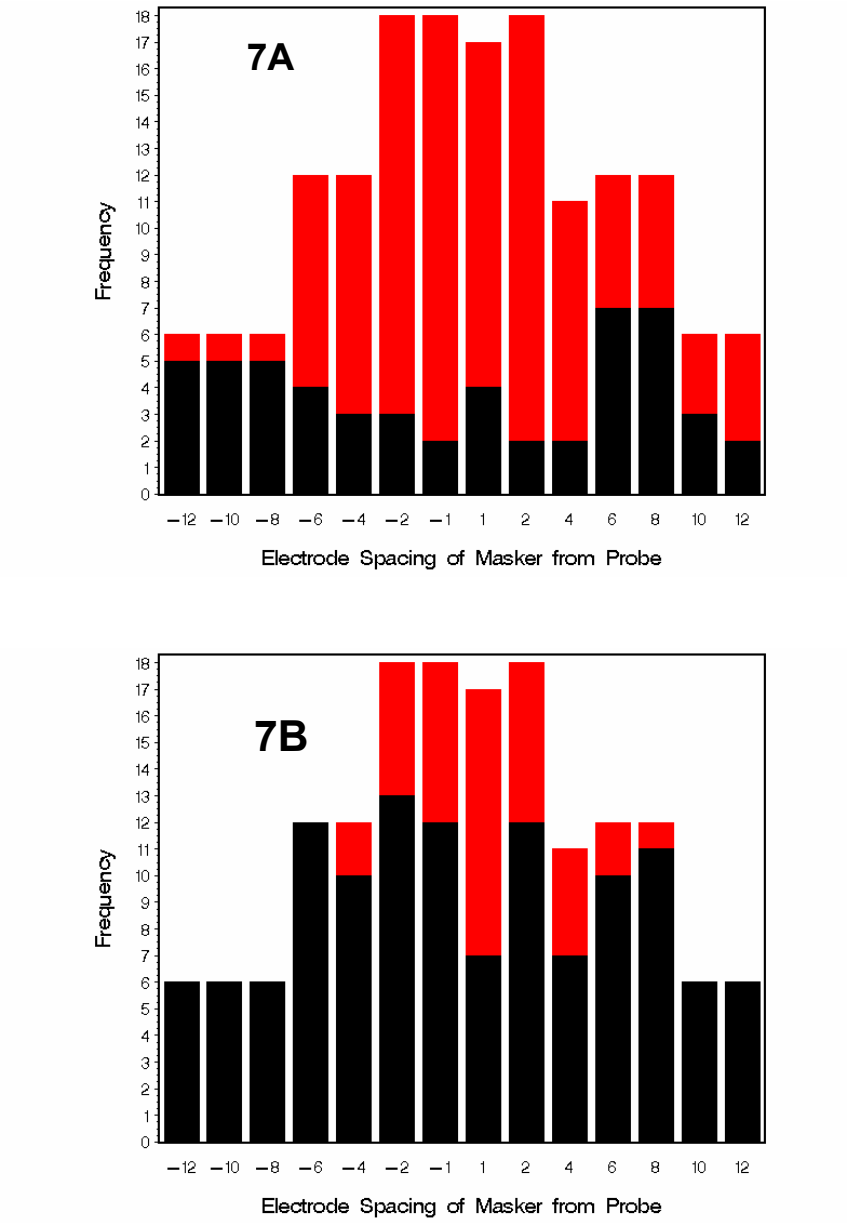

Figure 7. Frequency of IEP interaction across subjects and probe electrodes. The total bar height indicates the number of probe-masker combinations tested. The x-axis represents the distance between probe and masker electrodes in units of the longitudinal distance between neighboring electrodes (approximately 1 mm);.negative numbers indicate electrode configurations where the masker electrode is apical to the probe electrode (e.g., masker E6 and probe E7 are at -1 on this horizontal scale).. The black bar height represents the number of combinations not showing interaction and height of red bars represents the number of probe-masker combinations showing significant interaction Panel A shows results for in-phase conditions and panel B for out-of-phase conditions. The likelihood of interaction for any electrode configuration and phase condition is indicated by comparing the height of the red bar to that of the black bar

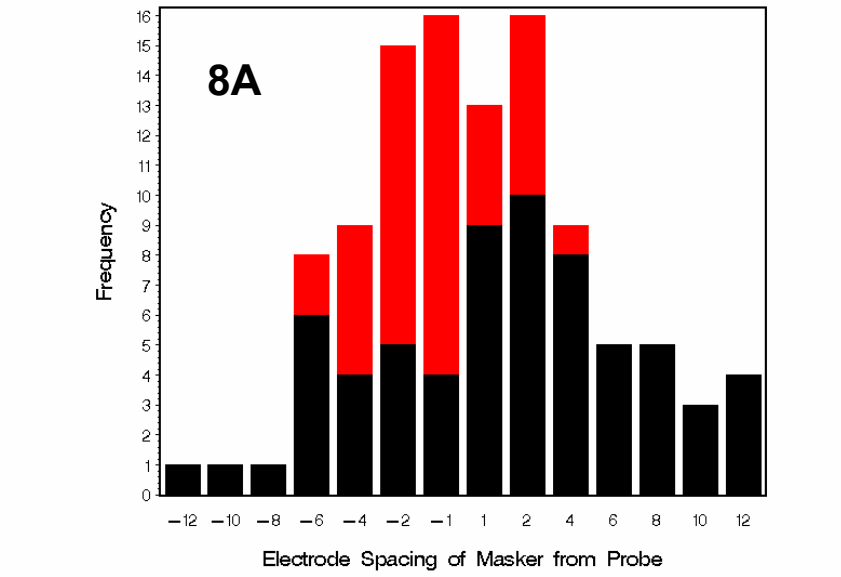

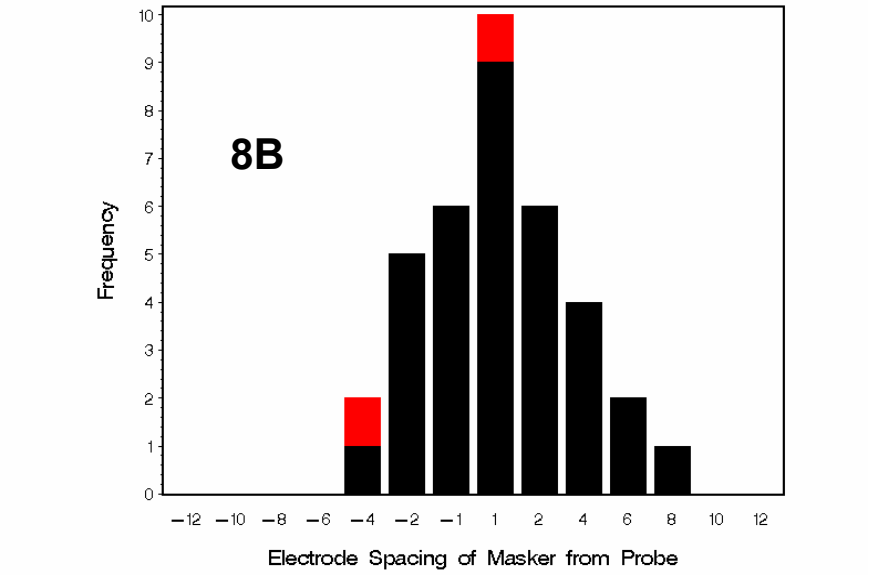

Figure 8. Frequency of "hyperinteraction". Axes are the same as in Figure 7. The total height of each bar indicates the number of measures showing significant interaction. The height of the black bars shows the number of measures showing significant interaction but not "hyperinteraction." The height of the red bars represents the number of measures where the degree of interaction was met the degree of "hyperinteraction". Panel A shows results for the in-phase conditions ($aIEP_C > aIEP_A$) and panel B for the out-of-phase conditions ($aIEP_D < aIEP_B$).

Figure 8 shows the frequency of the "hyperinteraction" condition where $aIEP_C > aIEP_A$ or $aIEP_D < aIEP_B$ (see example in panel D of Figure 6). The height of the black bars of Figure 8 indicates the number of measures where significant interaction was present but was not to the degree of "hyperinteraction". Red bar height shows the frequency of "hyperinteraction." Again, separate histograms have been generated for in-phase (panel A) and out-of-phase (panel B) maskers and the data have been collapsed across subjects and electrodes.

In general, across all test conditions, the difference between in-phase versus out-of-phase masker signals is greater for the frequency of "hyperinteraction" than for interaction in general (compare Figure 8 with Figure 7). There were only two occurrences (5%) of "hyperinteraction" with out-of-phase maskers. In contrast, 37% of all interaction occurrences with in-phase maskers reached the level of 'hyperinteraction'. "Hyperinteraction" was more likely when the masker electrode was close to the probe electrode and 79% of "hyperinteraction" observed occurred on maskers apical to the probe.

2.3.2 Frequency of IEP Interaction for Different Probe Electrodes

Figures 9 (in-phase conditions) and 10 (out-of-phase conditions) plot the frequency of interaction for each of the three probe electrodes studied. For in-phase maskers (Figure 9), the frequency of interaction is greatest for probe electrodes E3 and E7 with 77% and 73% of the experimental conditions showing interaction, respectively. The likelihood of interaction for these two probes is greatest for apical maskers and decreases with distance from the probe. While the likelihood of interaction also decreases with distance from the probe for E13, this probe electrode has fewer conditions showing interaction (48%) and the likelihood is greatest when the masker electrode is spaced two electrodes basal to the probe electrode.

For out-of-phase maskers (Figure 10), the frequency of interaction decreases as the probe electrode moves from apical to more basal locations. The likelihood of interaction is smallest for probe E13 with only 9% of the experimental conditions showing significant interaction compared to 31% and 27% for probes E3 and E7, respectively. Interestingly, the likelihood of interaction is greater for apical maskers only for probe E13, reversing the trend seen for in-phase maskers

Figure 11 shows that the trends observed in the frequency of "hyperinteraction" for in-phase maskers is also slightly different for probe E13 versus E3 and E7. For probes E3 and E7, nearly one-half of the interaction observed is larger than expected. (40% for probe E3 and 50% for probe E7). Also the majority of the "hyperinteraction" is observed for maskers apical to the probe (60% for probe E3 and 80% for probe E7). Only 15% of the interaction observed for probe E13 reached the level of 'hyperinteraction' and these measures are equally divided between apical and basal maskers.

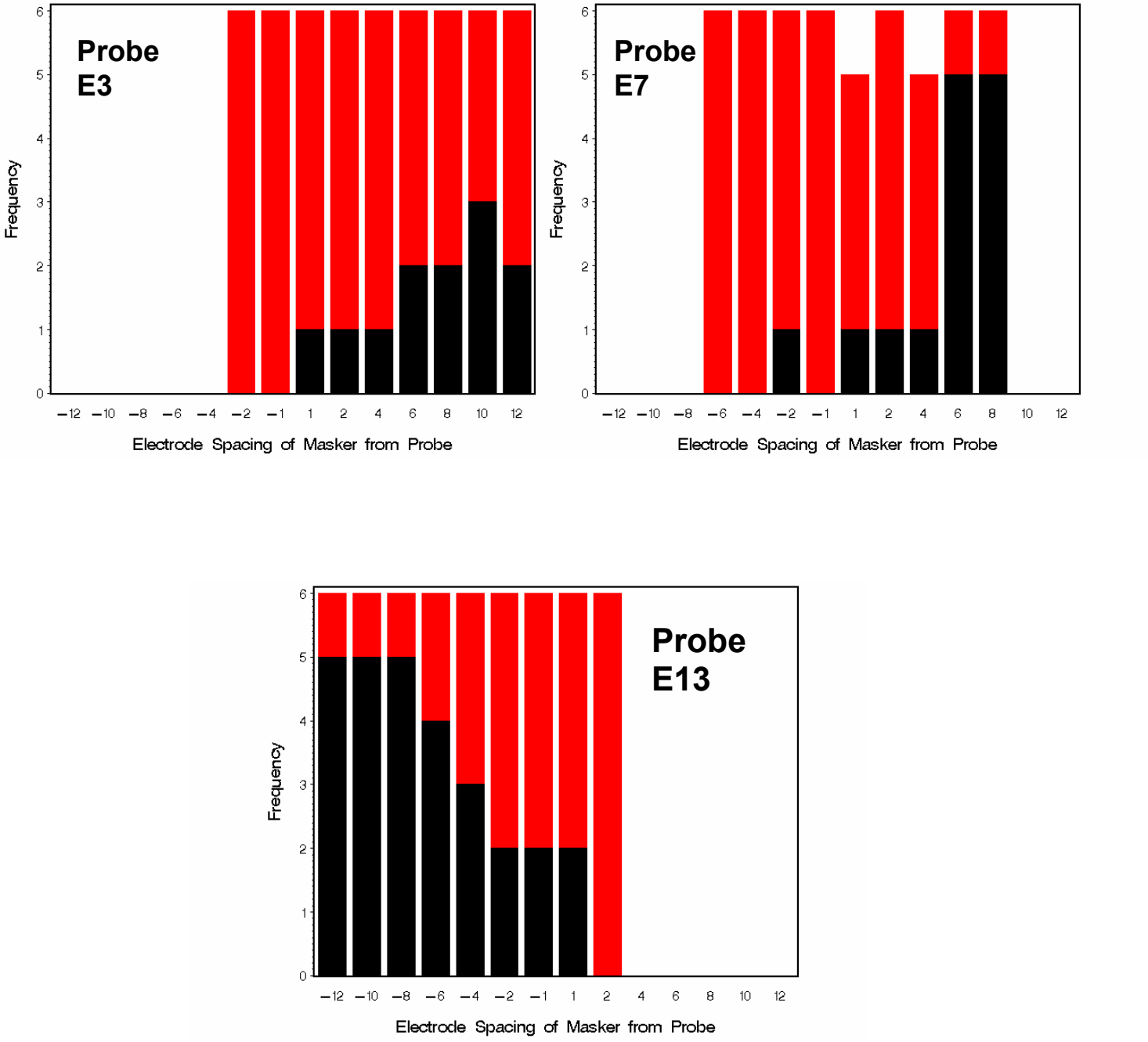

Figure 9. Frequency of no interaction (black bars) and significant interaction (red bars) for each of the probe electrodes across masker electrode and subjects for the in-phase conditions. Axes and bar assignments are as described for Figure 7.

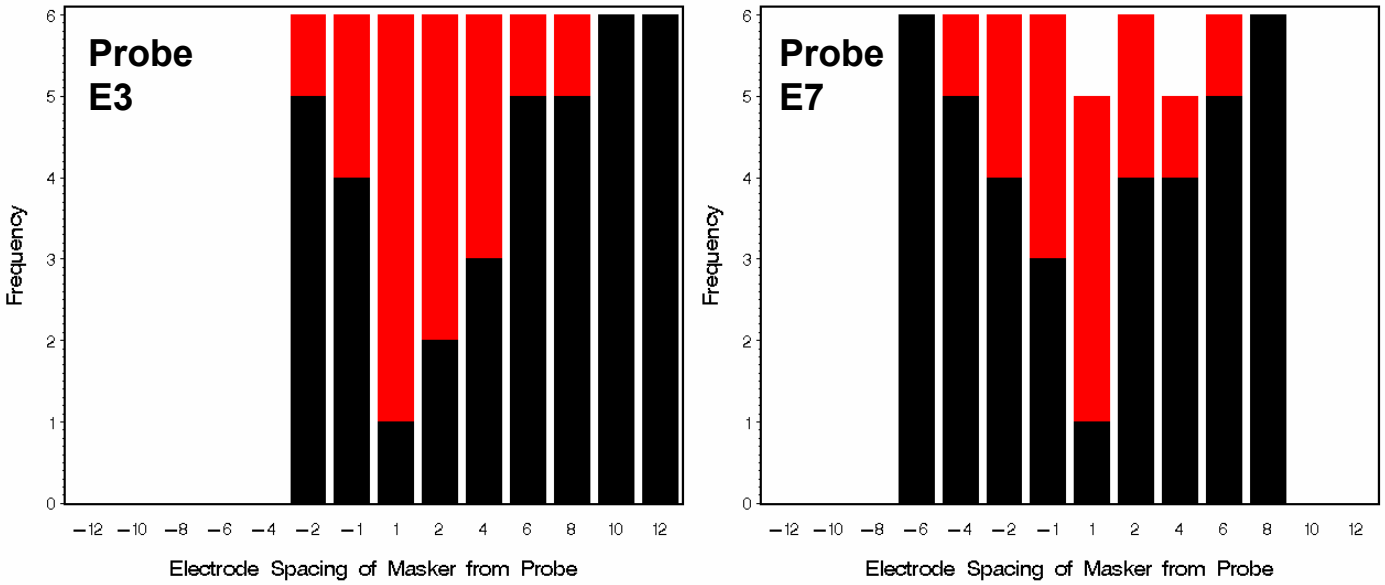

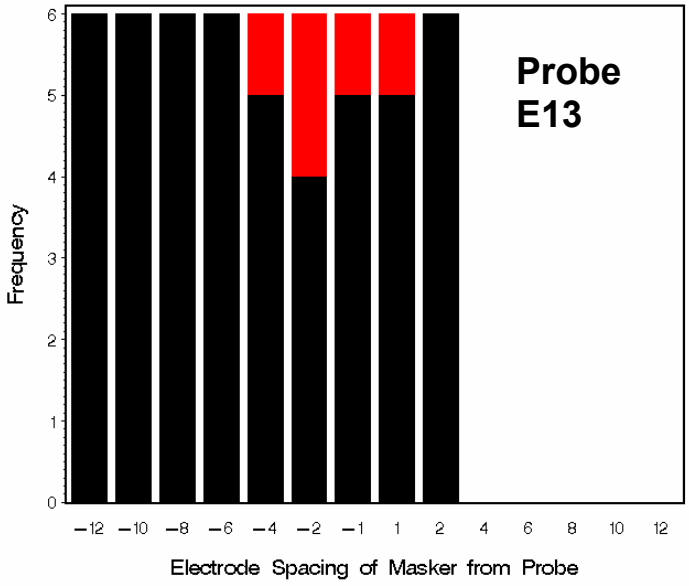

Figure 10. Frequency of no interaction (black bars) and significant interaction (red bars) for each of the probe electrodes across masker electrode and subjects for the out-of-phase conditions. Axes and bar assignments are as described for Figure 7.

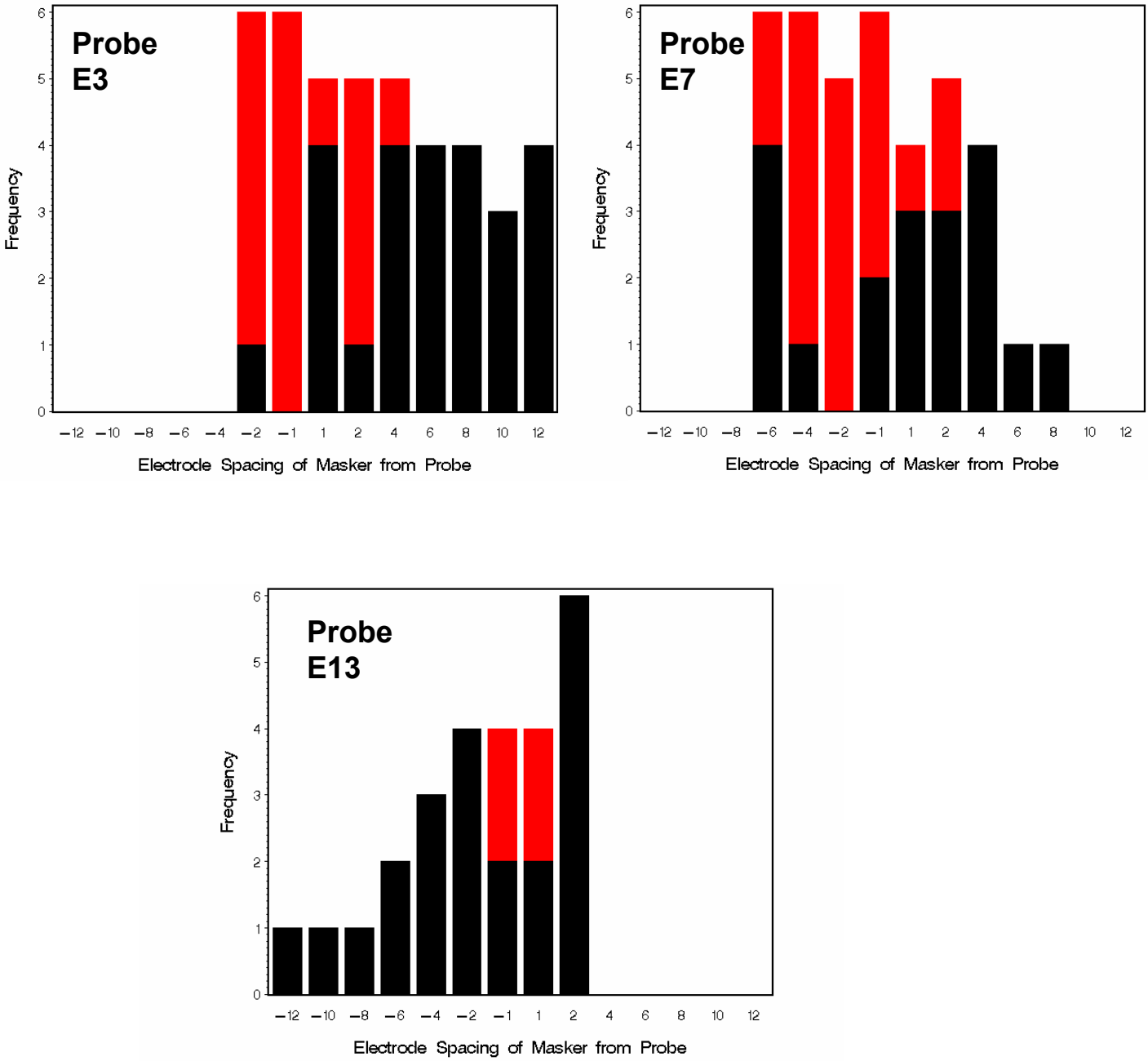

Figure 11. Frequency of in-phase measures showing significant interaction but not reaching the level of. "hyperinteraction" (black bars) vs. measures showing "hyperinteraction" for each of the probe electrodes across masker electrodes and subjects. Axes and bar assignments are as described for Figure 8.

There were only two occurrences of "hyperinteraction" for out-of-phase probes, one for a basal masker on probe E3 and one for an apical masker for probe E13. Given the number of comparisons made for all conditions, these occurrences could be attributed to chance alone.

In summary, it appears that the likelihood of IEP interaction changes with the position of the probe electrode and with the phase of the masker stimulus. Probes E3 and E7 are the most similar having a greater frequency of interaction and "hyperinteraction" than probe E13. For in-phase maskers, the likelihood of interaction and "hyperinteraction" is greater for maskers closer to the probe and for maskers apical to the probe. Interaction is less likely for masker signals that are out-of-phase with the probe signal and least likely for the most basal probe, E13.

The asymmetric nature of the interactions measured (less likely for out-of-phase stimuli and for basal maskers) and the occurrence of "hyperinteraction" are intriguing trends that are difficult to explain. We are in the process of using our three-dimensional, anatomical model of the implanted cochlea (Girzon, 1987) to investigate the mechanisms responsible for these features of the data. Initial results are promising, but considerable more effort will be required before that analysis is complete.

2.3.3 Frequency and size of interaction for individual subjects.

While the observed trends in IEP interaction are present across this group of good implant users, there is variability between subjects in the pattern and size of interaction. We are currently exploring methods to quantify interaction in individual subjects that allow for meaningful comparison across subjects and with psychophysical measures. The results of these efforts will follow in a subsequent report.

3.0 Fast-recovery recording amplifier for far-field and surface artifact potentials.

This section describes the design and operation of the fast-recovery amplifier system used in this project for the recording of surface artifact potentials (Finley et al., 2003 - QPR7 of this project) and electrically-evoked brainstem responses (Finley et al., 2002 - QPR4 of this project). It is also used in our recording of IEP responses in that the back-telemetry subsection of the Clarion C-II implant employs a similar amplifier integrated into the implanted stimulator package (Eddington et al., 2002 - QPR2 of this project; Finley et al., 2002 - QPR4 of this project; Karunasiri and Finley, 2001). Studies using an earlier version of this system to record IEP responses from patients with direct percutaneous connection to their electrodes have been previously reported (Wilson et al., 1995a; Wilson et al., 1995b; Finley et al., 1997; Wilson et al., 1997). The amplifier system was originally developed by Chris van den Honert, Charles Finley and Blake Wilson under a previous NIH contract at Research Triangle Institute. The system was described in general terms in an earlier report (van den Honert et al., 1997). In response to technical questions and to facilitate use of the technology by others we provide additional details about the present system.

The amplifier was designed to allow recording of low-level biological potentials immediately (< 20 μs) following the occurrence of large electrical artifacts due to stimulation events. Conventional amplifier systems (i.e., multi stage, op-amp-based, linear designs) typically perform poorly in this situation due to a variety of factors, including low output slew rates, asymmetrical clipping of outputs due to large baseline offsets caused by amplification of direct current (DC) signal components (i.e., electrode interface battery potentials), limited bandwidth, and nonlinear asymmetrical recovery from hard saturation. The latter is the most severe phenomenon and can result in the complete loss of signal due to sustained saturation for extended periods (>100 μs to several ms depending on test conditions and choice of test device).

Figure 12 shows a block diagram of the fast-recovery amplifier system. The battery-powered system consists of a low-gain, differential preamplifier stage followed by a cascade of fast-recovery, low-gain stages. The final stage is an optically-coupled output driver to allow operation of the system with a floating ground to minimize ground loop noise and ensure patient safety. All stages are designed for wide-bandwidth operation, ranging from DC to approximately 300kHz. A variable number of low-gain stages may be included in the cascade to adjust overall system gain. The preamplifier stage also features an auto-zeroing circuit to remove any standing DC offset potential appearing on the output of the preamplifier. The most significant source of this offset potential is the amplification of the net sum of the DC potentials appearing in the electrode/tissue interfaces. These potentials are quite variable and may drift during the course of recording. Consequently, the auto-zeroing circuit may be enabled and disable via an optically-coupled control signal as needed during recording.

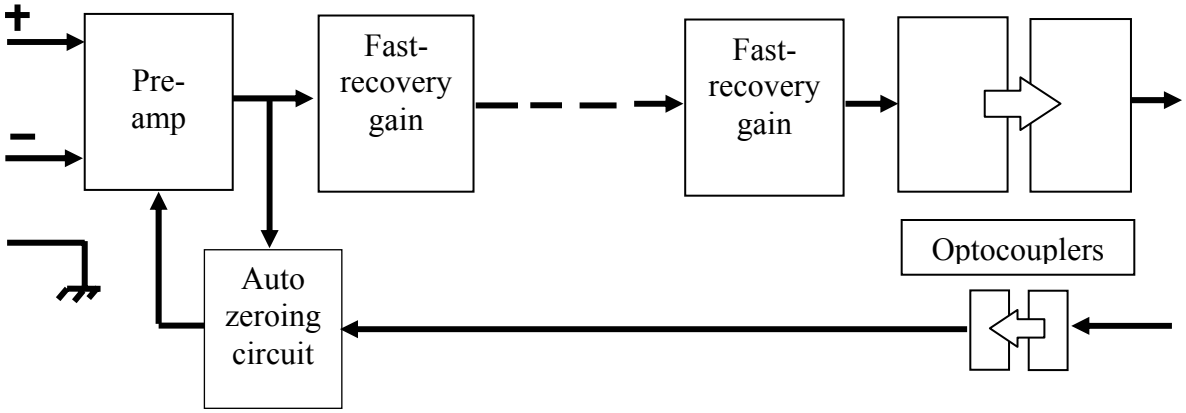

Figure 12. Block diagram of the fast-recovery amplifier system. See text for explanation.

The input preamplifier design is schematically shown in Figure 13. The preamp is configured with a TI (Burr-Brown) INA110 instrumentation amplifier (i-amp) operating at a gain of 10 with ±15-volt supplies. This FET-coupled-input device features high input impedances and fast settling times of 2 μsec to 0.1% at a gain of 10. At this gain the i-amp's bandwidths are 2.5 MHz for small signals and 270 kHz for large signals. The common-mode-rejection ratio (CMRR) is >100 dB at DC and greatly facilitates reduction of common mode noise such as 50/60 Hz interference and broadly distributed biological potentials appearing on the scalp (e.g., EMG).

CMRR typically diminishes at higher frequencies due to parasitic capacitances in board and device layout.

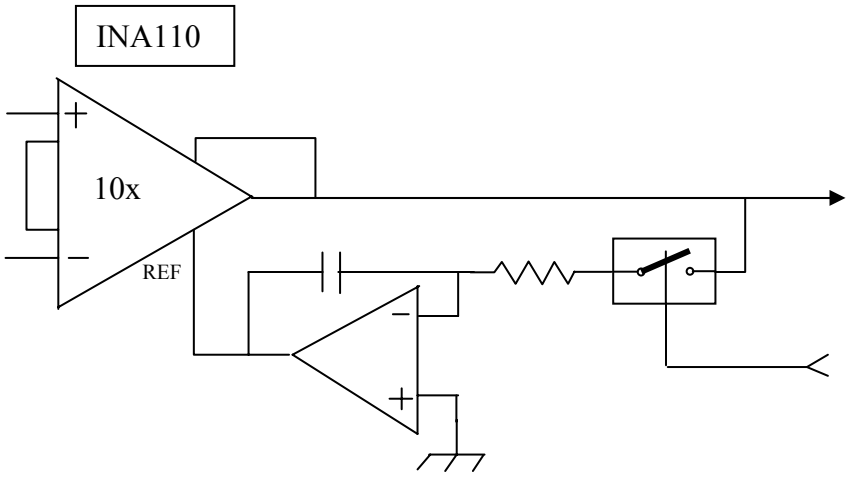

Figure 13. Basic preamplifier/auto-zeroing circuit.

DC electrode potentials appearing differentially on the inputs may produce a DC output offset as high as ±5 volts while operating with a gain of 10. Low-level biological potentials would be riding atop this DC pedestal. However, these potentials would be lost by the following gain stages due to amplifier saturation caused by amplification of the large DC offset. Consequently, a servo-based, auto-zeroing circuit is included to remove the DC offset on the preamp output. This circuit works by driving the reference input to the i-amp with an error signal derived by low-pass filtering the preamplifier's output. The error signal on the reference input forces subtraction of the low-pass signal from the output, thus giving the i-amp a high-pass characteristic without directly placing filters in the forward path of the amplifier. This is a common technique described widely in the instrumentation amplifier literature to allow shaping of i-amp pass-band characteristics while maintaining high input impedances and CMRR. The servo-loop has been modified with the addition of a FET-switch, which essentially makes the auto-zeroing circuit function as a "track-and-hold" device. When the switch is closed, the feedback path "tracks" the preamp output and functions as described previously to eliminate the DC output. When the switch is opened, the feedback path is interrupted, and the auto-zeroing op-amp "holds" steady at its output level at the time the switch was opened. During the "hold" mode the high-pass, cut-off frequency of the i-amp effectively extends to DC (zero frequency). During typical recording situations, the auto-zeroing circuit may be dynamically switched to "track" during periods when no stimulation and recording is occurring, then to "hold" for data collection.

The merit of the above approach is that the disruptive effects of large magnitude artifacts are minimized if the recording pathway has wide bandwidth, large dynamic range, and no reactive components to hold residual charge. Wide bandwidth recording is important in maintaining sharply rising and falling edges of electrical artifact potentials and thus prevents temporal

smearing of the artifact event into the desired recording window that immediately follows the artifact. Having a large dynamic range helps to minimize saturation effects during artifacts with high gain recording. Minimization of reactive components also reduces long-duration, low-level, exponentially-decaying residual after potentials following artifacts with imperfect net-zero charge balancing. In the typical recording situation there is, however, significant shunt capacitance in the tissue that tends to prolong artifact duration. This contamination must be addressed through post-processing techniques such as summed alternation averaging or scaled-template subtraction (Eddington et al.,2002 - QPR 2 of this project).

The design of the subsequent fast-recovery gain stages follow these principles in general but primarily seeks to resolve the problems created by hard saturation of active electronics during artifact events. Hard saturation of active, op-amp-based circuits results in prolonged and unpredictable recovery behavior due to local heating effects on the chip substrate. The fast-recovery stages address this problem by avoiding situations where saturation may occur. Figure 14 shows the basic gain stage used in the system. An INA110 i-amp is configured for a 10x gain. The input signal is soft clipped by a pair of parallel-connected, back-to-back signal diodes such that input signals greater than ±0.5 volts are gradually clipped as the forward-biased diode of the pair begins to conduct. Effectively, the diodes form a voltage divider with the series-connected 10 kohm resistor. As one of the diodes begins to conduct, its effective impedance is reduced, thus increasing the voltage division ratio with the 10 kohm resistor and allowing less instantaneous signal to pass through to the i-amp. For signals levels less that ±0.5 volts the diode pair has higher net impedance, thus creating less voltage drop with the 10 kohm resistor. The result is that small signals pass through the system in a linear manner and are amplified by the 10x i-amp. Large signals (i.e. electrical artifacts) are clipped at about ±0.5 volts, then amplified by 10 to produce ±5 volts on the i-amp output. This output level during the artifact event is well within the linear operating range of the i-amp; consequently, hard saturation of the active device is avoided and the i-amp can recover from the artifact in its normal fast settling time (≈ 2 μsec). By cascading several such stages together, low-level signals are linearly amplified by each stage, whereas the large artifacts are repeatedly clipped to ±0.5 volts and then amplified to ±5 volts by each stage. Because the back-to-back diodes have finite impedances even for small signals, there is some degree of attenuation by the resistor-diode divider. Consequently, the actual gain of each fast-recovery stage maybe less than the 10x expected from the i-amp gain setting and should be determined experimentally using a known source.

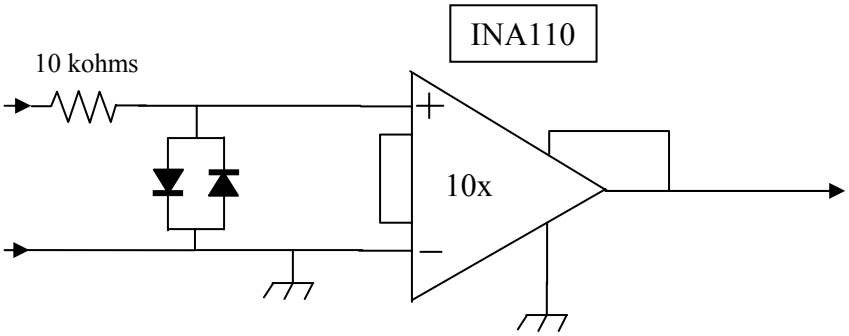

Figure 14. Basic fast-recovery, gain stage circuit.

The final, optically-coupled output stage is built around an Agilent HCNR201 high-linearity analog opto-coupler that features two matched photodetector diodes driven by a common light-emitting diode source. One detector is used to carry the forward path signal and the other is used in a feedback loop to stabilize the forward path gain. The implementation generally follows that recommended in the technical data sheet for the device.

Figure 15 shows a schematic circuit diagram for a three-stage, fast-recovery amplifier, including the preamplifier stage with autozeroing circuitry. Total gain for the amplifier is fixed at 1000 (3 x 10). The auto zeroing circuit is controlled by a separate logical control signal applied to PD5. The amplifier input lines are over-voltage protected with current limiting resistors (R4 and R5) and clamping diodes (D1-D4). Capacitors (C2-C11) are standard 0.1 μF ceramic bypass capacitors that are placed physically close to the active components. All parts are standard, readily available components.

Additional improvements to the design are being considered. One is the use of actively-driven guards on the input leads. Another is the addition of an actively-driven, common-mode ground for the test subject ground lead. Another is improved front-end and power-supply filtering to reduce susceptibility to radio frequency interference (RFI) encountered with implant system transcutaneous links.

Figure 15. Schematic of three-stage, fast-recovery amplifier.

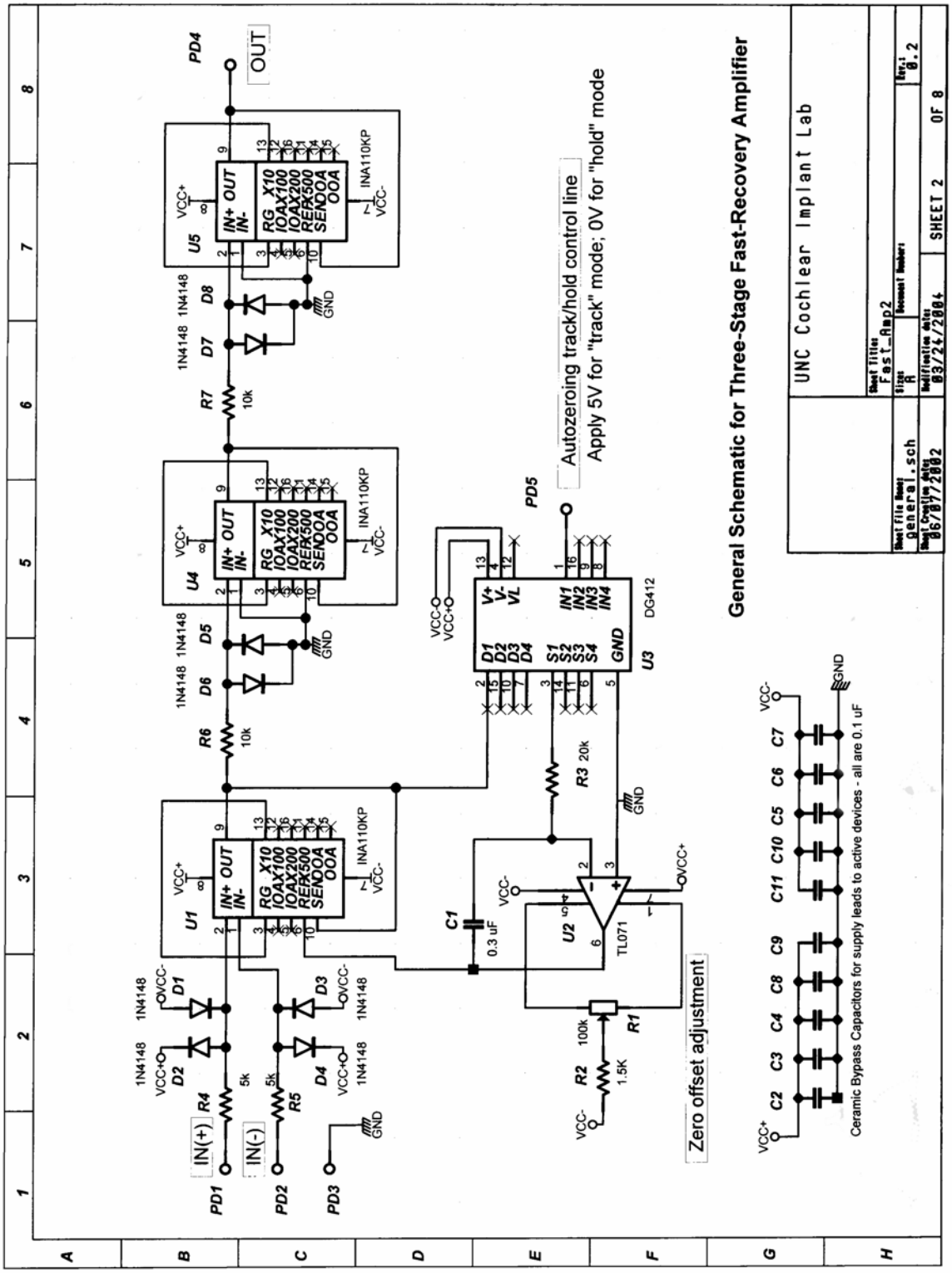

3.0 Future Work

We continue to measure relative interaural pitch, fusion, ITD-JND, speech reception, localization and binaural interactions in electrically-evoked brain stem responses as a function of time in the three bilaterally-implanted subjects described in earlier QPRs. We are also evaluating split-spectrum processors using asynchronous sound processors. These data, together with results from current testing designed to determine the cues these subjects use in localization tasks will be reported in future QPRs.

We are also continuing our work directed at triphasic stimulation waveforms. We have finished collecting psychophysical measures that compare interaction for biphasic and triphasic stimuli in subjects implanted with the Clarion CII/HiFocus implant system. The results show an advantage for triphasic stimulation. We have implemented a CIS sound-processing strategy employing triphasic carriers in wearable form for a number of subjects. These longitudinal studies of speech reception will soon be completed and their results reported in a future QPR.

Measurements of channel interaction using intracochlear evoked potentials (IEPs) are continuing. Now that measures using simultaneous stimulation are nearing completion, we plan to move to the interleaved-pulses stimulus condition. We are also beginning to compare the results of these IEP measures with similar behavioral measures made in the same subjects.

5.0 References

(Note: the referenced NIH quarterly progress reports can be found at: http://scientificprograms.nidcd.nih.gov/npp/qpr/auditory/qpr_auditory.html.)

Eddington, D.K., Herrmann, B., Finley, C.C. 2002. Speech processors for auditory prostheses: second quarterly progress report. Contract N01-DC-2-1001. Neural Prosthesis Program, National Institutes of Health, Bethesda.

Efron, B., Tibshirani, R.J. 1993. An Introduction to the Bootstrap, Chapman & Hall, New York.

Finley, C.C., Herrmann, B., Eddington, D.K., Noel, V., Tierney, J., Whearty, M. 2002. Speech processors for auditory prostheses: fourth quarterly progress report. Contract N01-DC-2-1001. Neural Prosthesis Program, National Institutes of Health, Bethesda.

Finley, C.C., Christopher, P., Eddington, Herrmann, B. 2003. Speech processors for auditory prostheses: seventh quarterly progress report. Contract N01-DC-2-1001. Neural Prosthesis Program, National Institutes of Health, Bethesda.

Finley, C.C., Herrmann, B., Eddington, D.K., Noel, V., Tierney, J., Whearty, M. 2002. Speech processors for auditory prostheses: fourth quarterly progress report. Contract N01-DC-2-1001. Neural Prosthesis Program, National Institutes of Health, Bethesda.

Finley, C.C., Wilson, B.S., van den Honert, C., Lawson, D.T. 1997. Speech processors for auditory prostheses: sixth quarterly progress report. Contract N01-DC-5-2103. Neural Prosthesis Program, National Institutes of Health, Bethesda.

Girzon, G. 1987. Investigation of Current Flow in the Inner Ear During Electrical Stimulation of Intracochlear Electrodes. S.M., M.I.T., Cambridge, MA.

Karunasiri, T. and Finley, C.2001. United States Patent 6,195,585. Remote monitoring of implantable cochlear stimulator. Issued February 27, 2001.

van den Honert, C, Finley, C.C.,. Wilson, B.S. 1997. Speech processors for auditory prostheses: ninth quarterly progress report. Contract N01-DC-5-2103. Neural Prosthesis Program, National Institutes of Health, Bethesda.

Wilson, B.S., Zerbi, M., Finley, C.C., Lawson, D.T., van den Honert, C.1997. Speech processors for auditory prostheses: eight quarterly progress report. Contract N01-DC-5-2103. Neural Prosthesis Program, National Institutes of Health, Bethesda.

Wilson, B.S., Finley, C.C., Zerbi, M., Lawson, D.T. 1995a. Speech processors for auditory prostheses: seventh quarterly progress report. Contract N01-DC-2-2401. Neural Prosthesis Program, National Institutes of Health, Bethesda.

Wilson, B.S., Finley, C.C., Zerbi, M., Lawson, D.T. 1995b. Speech processors for auditory prostheses: eleventh quarterly progress report. Contract N01-DC-2-2401. Neural Prosthesis Program, National Institutes of Health, Bethesda.